LECTURE 7: Phase transitions

1° Basic concepts and definitions:

ENTROPY–ENERGY ARGUMENT

$F = E - TS$

is minimized!

THE ROLE OF THERMODYNAMIC LIMIT

$Z = \mathrm{Tr} e^{-\beta \hat{H}} = \sum_n e^{-\frac{E_n}{k_B T}}$ — one Hamiltonian

Z = analytic function for $n < \infty$

$n \to \infty$ → gas, liquid, solid } many phases

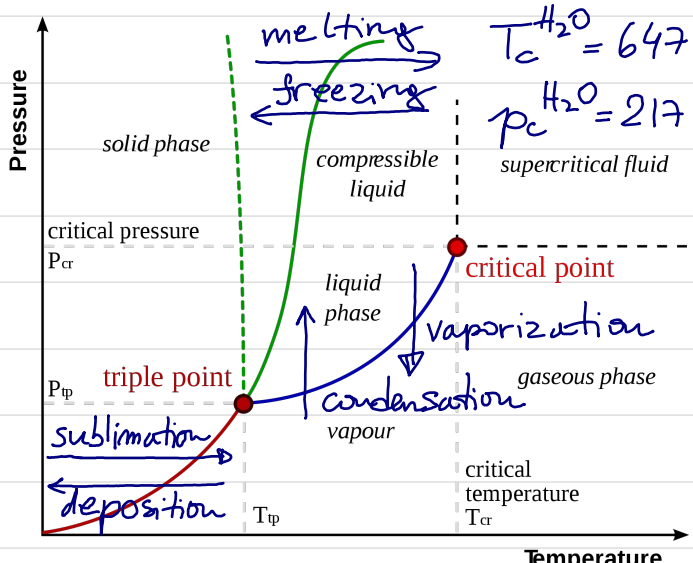

$T_c^{H_2O} = 647\ K$

$p_c^{H_2O} = 217.7\ atm$

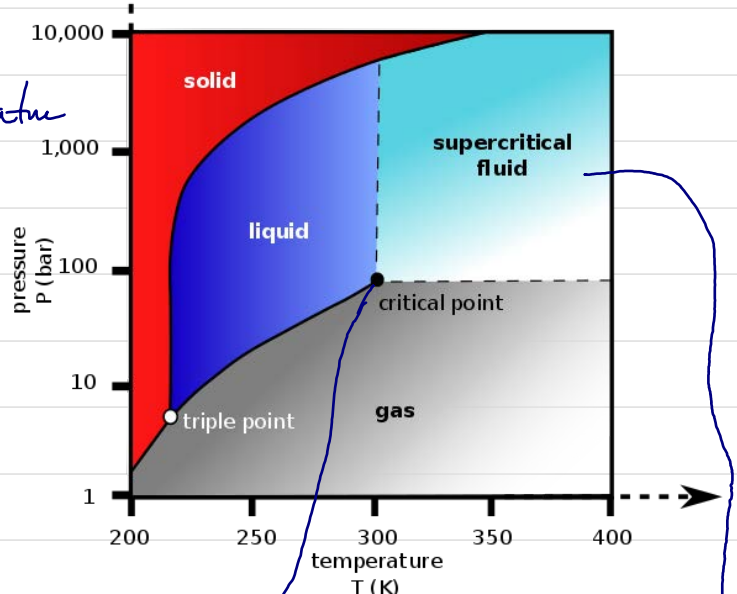

order parameter is thermodynamic variable: $\rho_{liquid} - \rho_{gas} = \begin{cases} 0, & T > T_c \\ \neq 0, & T < T_c \end{cases}$

$\beta = \begin{cases} 0.34 & CO_2 \\ 0.362 & Ar \\ 0.35 & Xe \end{cases}$

$t = \frac{T - T_c}{T_c}$ → reduced temperature

Supercritical CO_2

$T_c = 304.13\ K$, $p_c = 72.8$ atm

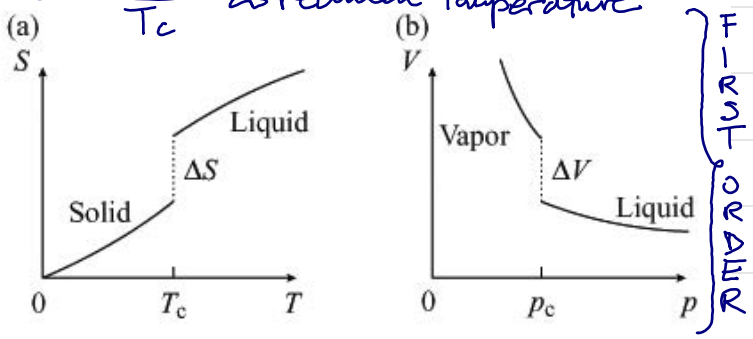

FIRST ORDER

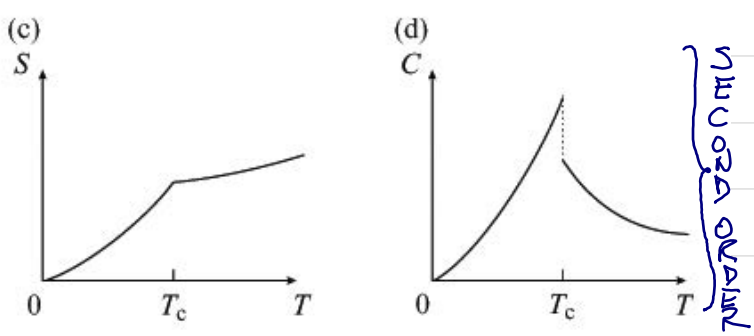

SECOND ORDER

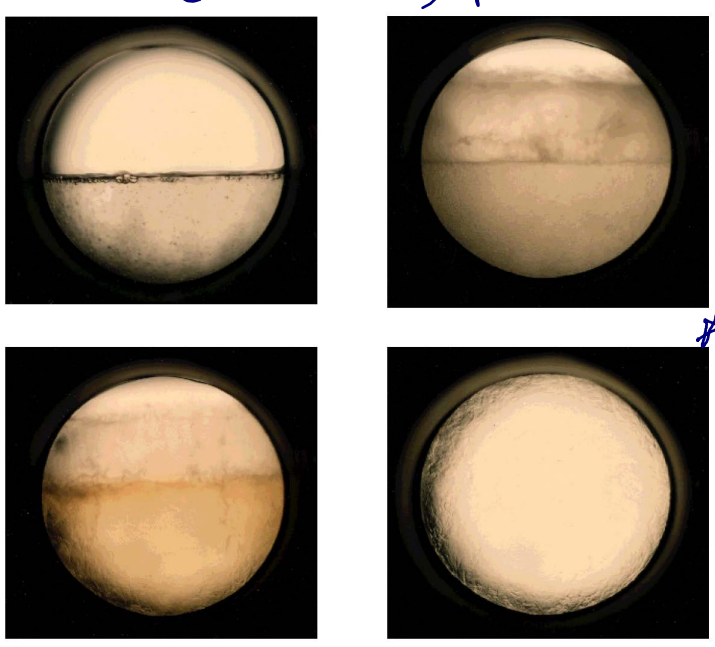

2° Examples from low to high energy physics

i) condensed matter physics

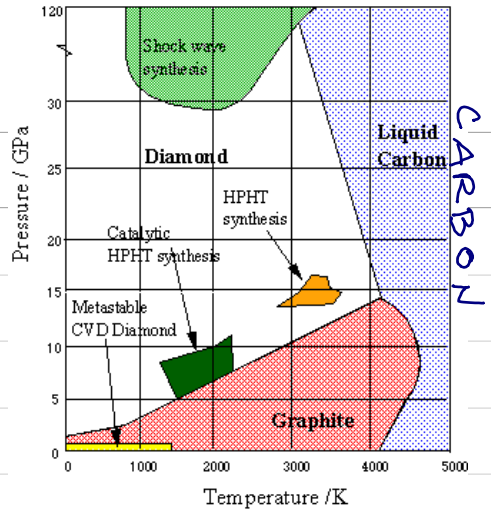

^{4}He

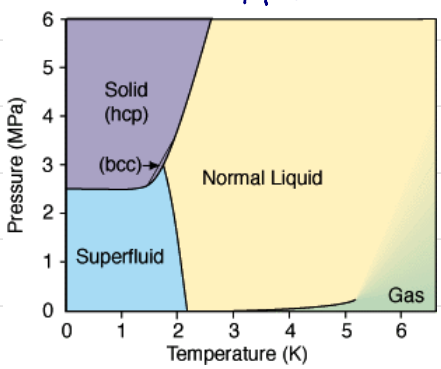

^{3}He

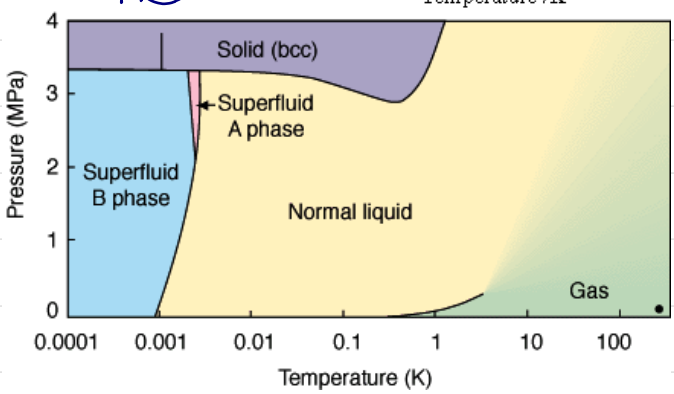

Rep. Prog. Phys. **82** (2019) 076901 Review

ii) QCD (quantum chromodynamics)

Rep. Prog. Phys. **82** (2019) 076901

Table 1. List of key times in the early Universe in terms of temperature, redshift and time. We are assuming the reheating temperature was sufficiently high and that each phase transition occurred in a single step. A large baryon chemical potential in the early Universe can also change the time of the QCD phase transition slightly and the temperature at which the electroweak phase transition occurs has some model dependence.

	T (GeV)	t (s)
Electroweak transition	∼20–200	10^{-11}
QCD transition	10^{-1}	10^{-4}
Big bang nucleosynthesis	$\times 10^{-4}$	10^{2}
Recombination	10^{-10}	10^{12}

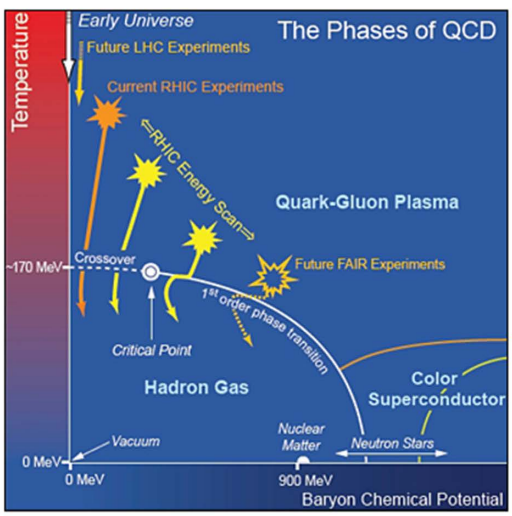

Figure 12. Phase diagram of QCD as a function of temperature and baryon chemical potential. Note that in the absense of a large chemical potential the QCD is expected to have a crossover transition. Reproduced from [294] with permission.

iii) cosmology

Rep. Prog. Phys. **82** (2019) 076901 Review

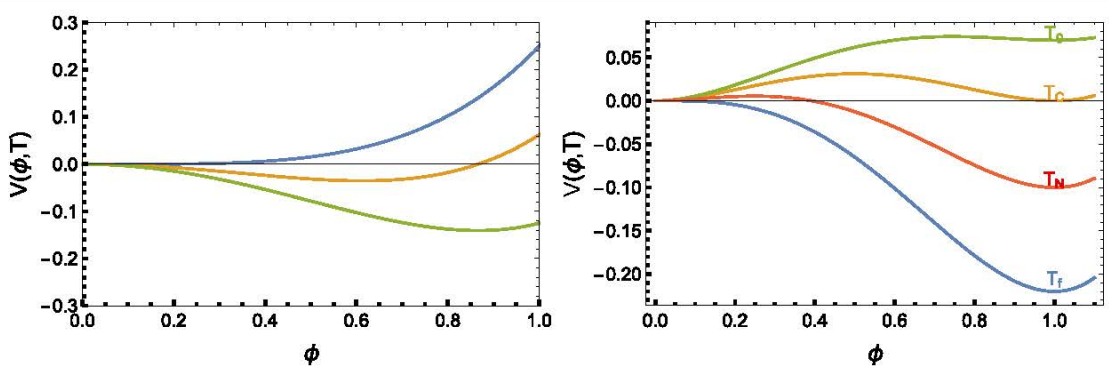

Figure 1. Evolution of an example potential with temperature with a 2nd order phase transition given in the left panel and 1st order phase transition in the right. The point where a new minimum appears away from the origin is called T_0. The critical temperature where the minima are degenerate is T_C. The nucleation temperature defined as the time where there is at least one critical bubble per Hubble volume is given by T_N and the temperature at which the phase transition completes is denoted T_f.

iv) magnetic materials

thermodynamics of magnetism:

$dE = \delta Q - \delta W = \delta Q + \delta W_{ext}$; $-pdV$ for mechanical systems

δW_{ext} using PHYS 208 concepts:

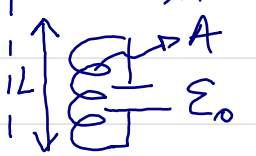

E | δQ | δW_{ext}

$RI = \mathcal{E}_0 - \mathcal{E}_{ind} \Leftrightarrow \mathcal{E}_0 I dt = RI^2 dt - \mathcal{E}_{ind} I dt$

$\mathcal{E}_{ind} = -d\Phi/dt = -AL n\, dB/dt$

$\delta W_{ext} = -\mathcal{E}_{ind} I dt = AL n I dB = V H dB$ (Ampere theorem)

$H = B/\mu_0 - M/V \Rightarrow \delta W_{ext} = \mu_0 V H dH + \mu_0 H dM$

→ generalization to inhomogeneous and noncollinear fields:

$$\delta W_{ext} = \int_V (\mu_0 \vec{H} \cdot d\vec{H})\, dV + \int_V \mu_0 \vec{H} \cdot d\vec{M}/V\, dV$$

↳ work of external agents to change $\vec{H} \mapsto \vec{H} + d\vec{H}$ & $\vec{M} \mapsto \vec{M} + d\vec{M}$ reversibly, so it can be applied only to monodomain ferromagnets

$$d\left(E - \int \frac{\mu_0 H^2}{2} dV\right) = \delta Q + \int_V \left(\mu_0 \vec{H} \frac{d\vec{M}}{V}\right) dV$$

↓ energy of magnet itself

$dE'_{mat} = \delta Q + \mu_0 H dM \Rightarrow \begin{cases} p \mapsto H \\ V \mapsto -M \end{cases}$

$dF'_{mat} = -SdT + H dM$

$E_{mat} = E'_{mat} - \mu_0 \vec{H} \cdot \vec{M}$ ↳ potential energy of $\vec{M}$ in $\vec{H}$

$F_{mat} = F'_{mat} - HM \Rightarrow dF_{mat} = -SdT - MdH$

Table II. Various free energies for the magnetostatic case. We have written the magnetic field part of the energy in terms of the separate contributions from the bound and free currents. In this way we clearly see that the different Hamiltonians and free energies differ as to which parts of the magnetic field energy, $(\frac{1}{2})\int dx(\mathbf{B}_b^2 + 2\mathbf{B}_b \cdot \mathbf{B}_{ext} + \mathbf{B}_{ext}^2)$, are included. The first entry in the table is the most useful because it includes all the terms in the Hamiltonian associated with the system. Furthermore, the expression for δF_{mat} also gives the work done on the material if it is moved in the external field.

Hamiltonian	Free energy change
$\mathcal{H}_{mat} = \mathcal{H}_0(\{\mathbf{p} - q\mathbf{A}\}) + \frac{1}{2}\int dx \mathbf{B}_b^2$	$\delta F_{mat} = -\int_V dx \mathbf{M} \cdot \delta \mathbf{B}_{ext}$ [6,12]
$\mathcal{H}'_{mat} = \mathcal{H}_0(\{\mathbf{p} - q\mathbf{A}\}) + \frac{1}{2}\int dx \times (\mathbf{B}_b^2 + 2\mathbf{B}_b \cdot \mathbf{B}_{ext})$	$\delta F'_{mat} = \int_V dx \mathbf{B}_{ext} \cdot \delta \mathbf{M}$ [6,8,14]
$\mathcal{H}_{comb} = \mathcal{H}_0(\{\mathbf{p} - q\mathbf{A}\}) + \frac{1}{2}\int dx \times (\mathbf{B}_b^2 + 2\mathbf{B}_b \cdot \mathbf{B}_{ext} + \mathbf{B}_{ext}^2)$	$\delta F_{comb} = \int dx \mathbf{H} \cdot \delta \mathbf{B}$ [3]
$\mathcal{H}_0(\{\mathbf{p} - q\mathbf{A}\})$	$\delta F_0 = -\int_V dx \mathbf{M} \cdot \delta \mathbf{B}$

Free energies in the presence of electric and magnetic fields

Onuttom Narayan[a] and A. P. Young
Department of Physics, University of California, Santa Cruz, California 95064

(Received 14 April 2004; accepted 24 September 2004)

We discuss the different free energies and Hamiltonians for materials in static electric and magnetic fields and which choice is the most appropriate for statistical mechanics calculations. We also discuss the relation between the various free energies and the Landau function which has to be minimized to determine the equilibrium polarization or magnetization. © *2005 American Association of Physics Teachers.*

[DOI: 10.1119/1.1819934]

phase transitions in magnetic materials:

paramagnet $T>T_c$ ferromagnet $T<T_c$

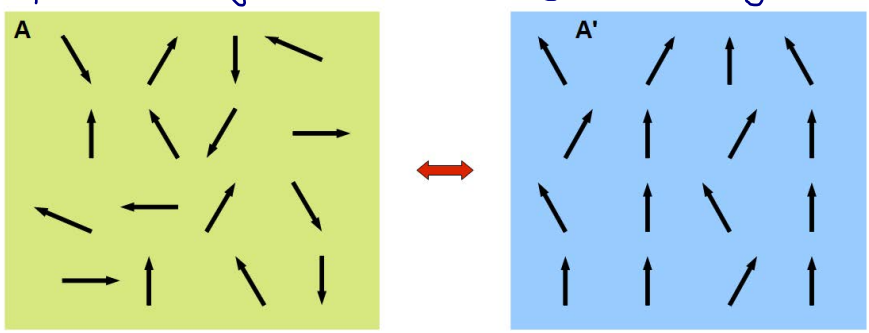

$\vec{M} = \sum_i \vec{\mu}_i = 0$ $\vec{M} = \sum_i \vec{\mu}_i \neq 0$

per atom

$m \Leftrightarrow$ order parameter

$m(T, h=0) = \begin{cases} 0, & T>T_c \\ |t|^{\beta}, & T<T_c \end{cases}$

$h \neq 0$

second order T_c T

$m(T=T_c) \propto h^{1/\delta}$

$m = \chi \cdot h + O(h^3)$ $T>T_c$

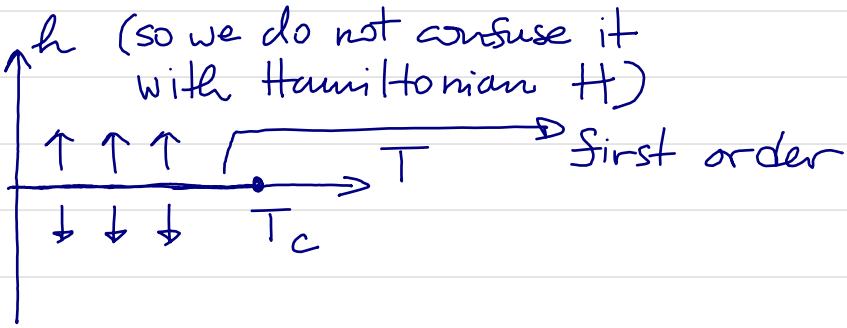

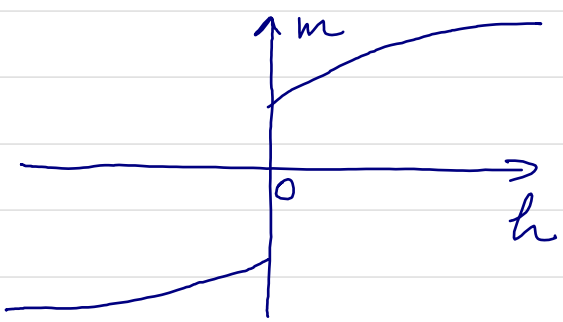

→ how to measure β & δ experimentally:

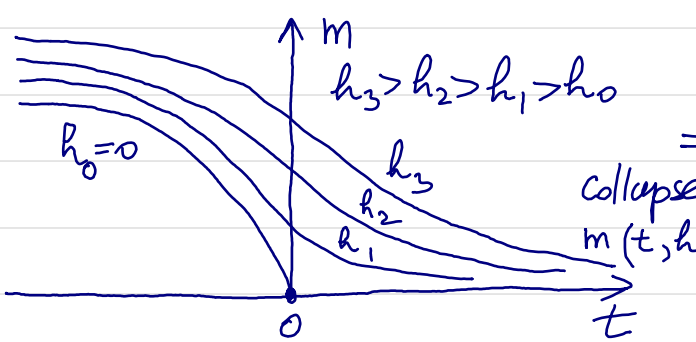

collapse to one curve

$m(t,h) = h^{1/\delta} g\left(\frac{t}{h^{1/\delta\beta}}\right)$

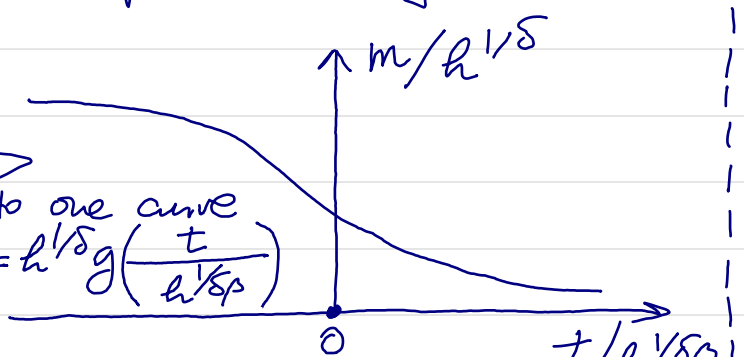

$\chi = (\partial m/\partial h)$

$\chi(T, h=0) \propto |t|^{-\gamma_\pm}$

$\gamma_+ \approx \gamma_-$

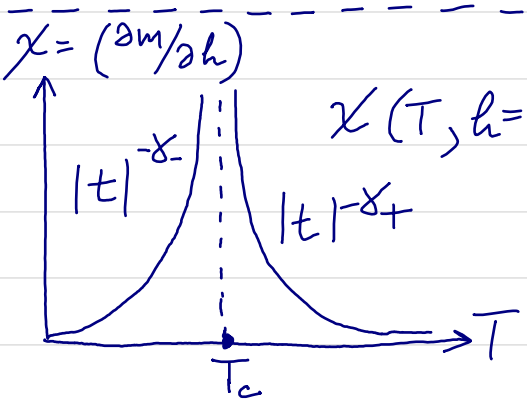

$C = (\partial E/\partial T)_m$

$C(T, h) = |t|^{-\alpha_\pm}$

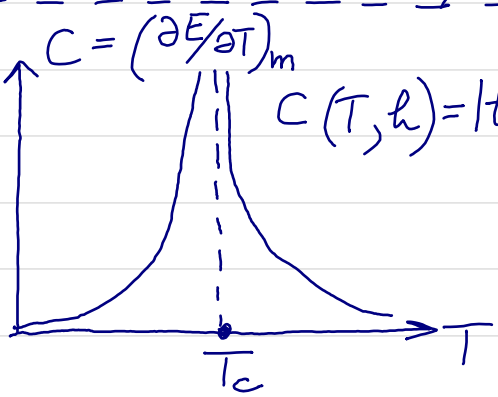

→ define critical exponents via:

$$\alpha = \lim_{t \to 0} \frac{\ln |f(t)|}{\ln |t|}$$

which gives $\alpha \neq 0$ for power laws or $\alpha = 0$ for log divergence

→ higher order terms:

$$\chi = A|t|^{-\gamma} + \underbrace{B|t|^{-\gamma+1}}_{\text{weaker singularity}} + \ldots + \text{const.} + \underbrace{t + t^2 + \ldots}_{\text{regular terms}}$$

→ exponents are connected: $\underbrace{\alpha + 2\beta + \gamma = 2}_{\text{Rushbrooke scaling}}$
so theory should explain such relations

	T_c (K)	β	γ
Fe	1043	0,35	1,27
Co	1394		1,21
Ni	630	0.38	1.27
Gd	293		1.33
Dy	85		
	non-universal	universal	

→ use simplest model to capture universality
class of critical exponents which cannot depend on microscopic details

- UNIVERSALITY CLASS determined by:
  - symmetries of the system
  - range of interactions
  - dimensionality of space (i.e., how many neighbors) — connectivity

Mermin-Wagner theorem: Continuous symmetry cannot be SPONTANEOUSLY BROKEN at $T>0$ in system with sufficiently short-ranged interactions in spatial dimensions $D \leq 2$

→ state of the system has lower symmetry than its Hamiltonian

NEVERTHELESS, 2D MATERIALS & MAGNETS

REVIEW ARTICLE
https://doi.org/10.1038/s41565-019-0438-6
nature nanotechnology

Magnetic 2D materials and heterostructures

M. Gibertini[1,2], M. Koperski[3,4], A. F. Morpurgo[1,5] and K. S. Novoselov[3,4]*

The family of two-dimensional (2D) materials grows day by day, hugely expanding the scope of possible phenomena to be explored in two dimensions, as well as the possible van der Waals (vdW) heterostructures that one can create. Such 2D materials currently cover a vast range of properties. Until recently, this family has been missing one crucial member: 2D magnets. The situation has changed over the past 2 years with the introduction of a variety of atomically thin magnetic crystals. Here we will discuss the difference between magnetic states in 2D materials and in bulk crystals and present an overview of the 2D magnets that have been explored recently. We will focus on the case of the two most studied systems—semiconducting CrI_3 and metallic Fe_3GeTe_2—and illustrate the physical phenomena that have been observed. Special attention will be given to the range of new van der Waals heterostructures that became possible with the appearance of 2D magnets, offering new perspectives in this rapidly expanding field.

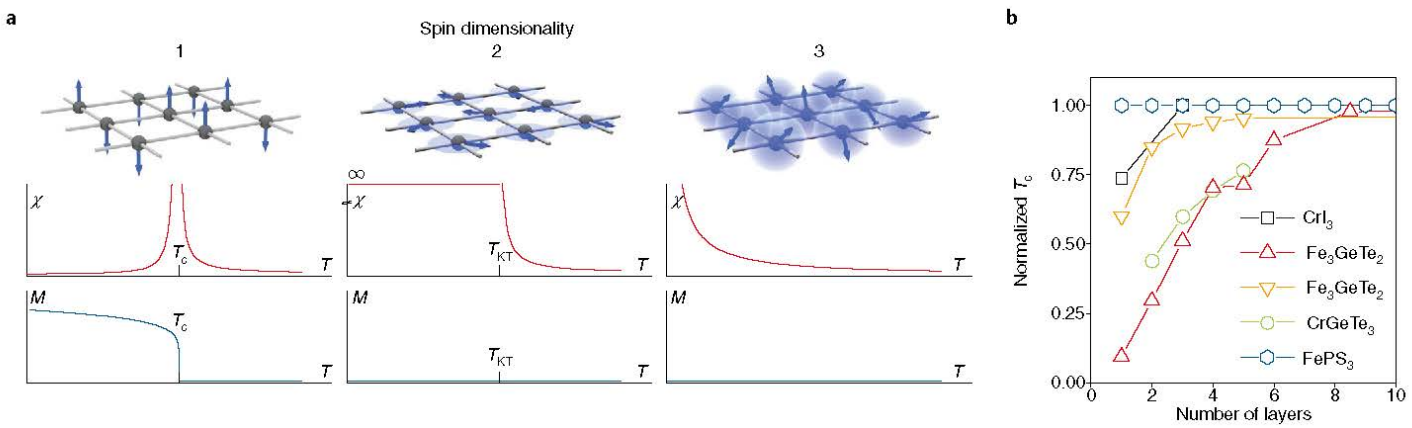

Fig. 1 | Role of spin dimensionality and evolution of T_c. **a**, A spin dimensionality $n = 1$ means that the system has a strong uniaxial anisotropy and the spins point in either of the two possible orientations ('up' or 'down') along a given direction. The system behaves effectively as if it had only a single spin component along the easy axis, and the underlying spin Hamiltonian for localized spins is called the Ising model. The case $n = 2$ corresponds to an easy-plane anisotropy that favours the spins to lie in a given plane, although the orientation within the plane is completely unconstrained. The spins can thus be considered to have effectively only two components (associated with the two in-plane directions), which are successfully described within the XY model. Note that in this case $\chi \to \infty$ for $T < T_{KT}$. Finally, for isotropic systems, $n = 3$ and there is no constraint on the direction of the spins. The underlying spin Hamiltonian in this case is the isotropic Heisenberg model. **b**, T_c (normalized to bulk T_c^{3D} for the particular material) as a function of the number of layers. Data for CrI_3 adapted from ref. [46], SNL; for Fe_3GeTe_2 (red curve), ref. [58], SNL; for Fe_3GeTe_2 (orange curve), ref. [54], SNL; for $CrGeTe_3$, ref. [47], SNL; for $FePS_3$, ref. [41], American Chemical Society.

Table 1 | Critical behaviour from 2D to 3D

Model	β	γ	ν	δ	T_c
	$M(T<T_c) \propto \lvert t\rvert^{\beta}$	$\chi \propto \lvert t\rvert^{-\gamma}$	$\xi \propto \lvert t\rvert^{-\nu}$	$M(T_c) \propto \lvert B\rvert^{1/\delta}$	
2D Ising	1/8	7/4	1	15	$2J/[k_B \ln(1+\sqrt{2})]$ (ref. [28])
3D Ising	0.3265	1.237	0.630	4.789	$T_c^{2D}(1 + C(J_L/J)^{4/7})$ (ref. [108])
3D XY	0.348	1.318	0.672	4.787	$T_{KT} + C\lvert J\rvert/[\ln(\lvert J/J_L\rvert)]^2$ (ref. [109])
3D Heisenberg	0.369	1.396	0.711	4.783	$C\lvert J\rvert/\ln(\lvert J/J_L\rvert)$ (refs. [110,111])
Mean field	0.5	1	0.5	3	$S(S+1)zJ(1 + z_L/zJ_L/J)/(3k_B)$ (ref. [112])

Critical exponents governing the behaviour of magnetization (M), susceptibility (χ) and correlation length (ξ) as a function of the reduced temperature, $t = T/T_c - 1$, or the magnetic field B, for different models in 2D and 3D. Not all the critical exponents are independent, as they are related by scaling relationships[113] such as $\gamma = \beta(\delta - 1)$ and $2\beta + \gamma = d\nu$, where d is the space dimensionality. Whereas the critical exponents for the 2D Ising model and mean-field theory can be determined analytically, for the other models they are results of numerical calculations[114]. In 2D, the critical exponents can be rigorously defined only for the Ising model, which is the only one displaying a standard phase transition to long-range order at finite T_c. Because long-range order in the 2D XY model is suppressed only in the thermodynamic limit, finite-size samples can sustain a non-vanishing magnetization, and its critical behaviour has been experimentally observed (for example in Rb_2CrCl_4 (ref. [115])), with a corresponding critical exponent[116] $\beta \approx 0.23$. For each model, an expression for the critical temperature T_c is also provided (C is a numerical coefficient, S is the spin on each site, and z and z_L are the intra- and interlayer coordination numbers, respectively), assuming in the 3D case a layered structure with $\lvert J_L/J\rvert \ll 1$ (see Box 1), where J is the intralayer and J_L the interlayer exchange coupling. In the case of the 2D Ising model, the argument of the logarithm depends on the lattice type, and the reported expression refers to a square lattice.

3° Quantum mechanics and Hamiltonians of ferromagnets exhibiting $\vec{M} \neq 0$ in $\vec{B}_{ext} = 0$

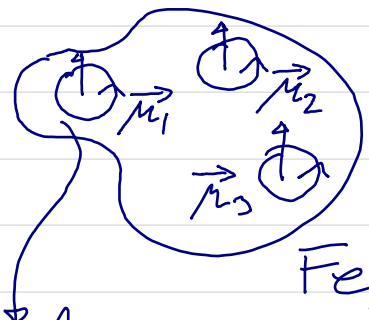

Fe_3O_4

3500 BC China → meteor iron
800 BC Greece → lodestone

Amper currents as generator of phenomenological magnetic moments in classical electrodynamics, but where is battery to supply Joule heat losses?

i) Bohr–van Leeuwen theorem → in classical physics no material can have nonzero $\vec{\mu}_i$

$$\vec{B}(\vec{r}) = \frac{\mu_0}{4\pi} \sum_{i=1}^{N} \frac{\vec{v}_i \times (\vec{r} - \vec{r}_i)}{|\vec{r} - \vec{r}_i|^3}, \quad \vec{B} = \nabla \times \vec{A}$$

$$H = \frac{1}{2m} \sum_i \left[\vec{p}_i - e\vec{A}(\vec{r}_i) \right]^2 + V(\vec{r}_1, \dots, \vec{r}_N)$$

$$Z = \frac{1}{N! \, \ell_Q^{3N}} \int d^3r_i \, d^3p_i \, e^{-\beta H}$$

$$\vec{p}_i \mapsto \tilde{\vec{p}}_i = \vec{p}_i - e\vec{A}(\vec{r}_i) \Rightarrow Z = \frac{1}{N! \, \ell_Q^{3N}} \int \underbrace{\frac{\partial(\vec{p}_1, \dots, \vec{p}_N)}{\partial(\tilde{\vec{p}}_1, \dots, \tilde{\vec{p}}_N)}}_{=1} d^3r_i \, d^3\tilde{p}_i \times e^{-\beta \left[\frac{1}{2m} \sum \tilde{\vec{p}}_i^{\,2} + V(\vec{r}_1, \dots, \vec{r}_N) \right]}$$

$$F = -k_B T \ln Z$$

$$\Downarrow$$

$$M = -\partial F / \partial B \equiv 0 \rightarrow$$ so no spontaneous magnetization in the absence of external $\vec{B}$

ii) Magnetic dipole moment due to orbital and spin degrees of freedom in QM

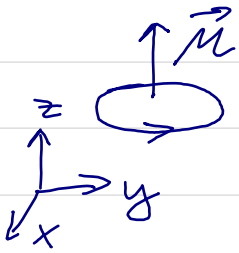

$$\vec{B} = \frac{\mu_0}{4\pi} \frac{3(\vec{\mu}\cdot\vec{r})\cdot\vec{r} - r^2\vec{\mu}}{r^5}$$

$$\vec{\mu}_L = \pi I R^2 \hat{z} = \frac{-e}{2m}\vec{L} .$$

orbital: $\hat{\vec{\mu}}_L = -\frac{e\hbar}{2m}\frac{\hat{\vec{L}}}{\hbar}$

$\frac{e\hbar}{2m} \equiv \mu_B$ is Bohr magneton, $= \frac{1}{137}$

spin: $\hat{\vec{\mu}}_S = -g\mu_B \frac{\hat{\vec{S}}}{\hbar}$, $g = 2.0023 = 2 + \frac{\alpha}{\pi} + O(\alpha^2)$

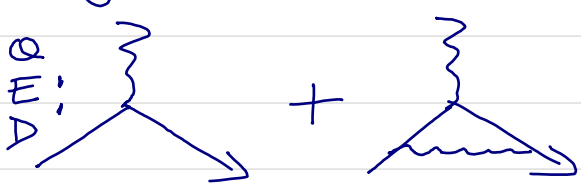

■ total magnetic dipole moment of ions:

$$\hat{\vec{\mu}}_J = \hat{\vec{\mu}}_L + \hat{\vec{\mu}}_S \approx -\mu_B\hat{\vec{L}} - 2\mu_B\hat{\vec{S}} = -\mu_B(2\hat{\vec{S}} + \hat{\vec{L}})$$

$$[\hat{H}, \hat{\vec{J}}] = 0, \quad \hat{\vec{J}} = \hat{\vec{L}} + \hat{\vec{S}} \qquad = -\mu_B(\hat{\vec{J}} + \hat{\vec{S}})$$

$[\hat{H}, \hat{\vec{S}}] \neq 0 \neq [\hat{H}, \hat{\vec{L}}]$ due to spin-orbit coupling $\lambda \hat{\vec{L}}\cdot\hat{\vec{S}}$

$[\hat{H}, \hat{\vec{\mu}}_J] \neq 0$ ⇒ so we cannot talk about sharp μ_J in energy eigenstates since $|E_n\rangle$ are not eigenstates of $\hat{\vec{\mu}}_J$ as well

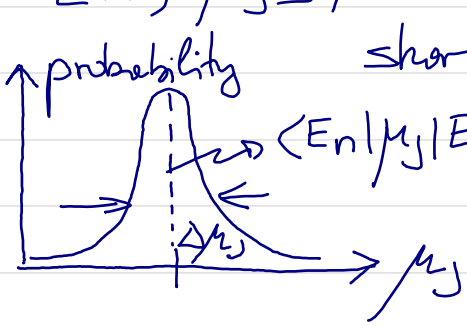

$$\vec{\mu}_{obs} = \frac{(\vec{\mu}_J \cdot \vec{J})\,\vec{J}}{\vec{J}\cdot\vec{J}} = -\mu_B \vec{J} + \frac{\mu_B}{2}\,\frac{(\vec{J}-\vec{S})^2 - \vec{J}\cdot\vec{S} - \vec{S}\cdot\vec{S}}{\vec{J}\cdot\vec{J}}\,\vec{J}$$

$$= -\mu_B \vec{J} - \frac{\mu_B}{2}\,\frac{J(J+1)+S(S+1)-L(L+1)}{J(J+1)}\,\vec{J}$$

$$= -g_J \cdot \mu_B \cdot \vec{J}$$

→ Landé g-factor: $g_J = 1 + \frac{J(J+1)+S(S+1)-L(L+1)}{2J(J+1)}$

- magnetic dipole moment of nucleons: $\vec{\mu}_N = g_N \mu_N \vec{I}$, $\mu_N = \frac{e\hbar}{2m_p}$, $1 < g_N < 10$

iii) dipole-dipole interaction could align $\vec{\mu}_i$ but it is too weak to produce observed T_c

$$V = -\vec{\mu}_2 \cdot \vec{B}_1(\vec{r}_2) = \frac{\mu_0}{4\pi}\,\frac{3(\vec{\mu}_1\cdot\vec{r})(\vec{\mu}_2\cdot\vec{r}) - r^2\,\vec{\mu}_1\cdot\vec{\mu}_2}{r^5}$$

$$k_B T_c \sim z \cdot \frac{\mu_0}{4\pi}\,\frac{\mu^2}{a^3} = z\,\frac{\mu_0}{4\pi}\,\frac{g^2\mu_B^2}{4a^3}$$

(a → lattice spacing; z ↑ no of nearest neighbors)

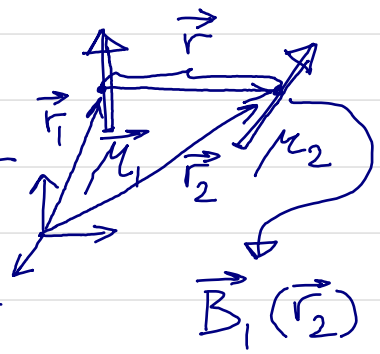

bcc Fe: $z = 8$, $a = 2.49\,\text{Å} \Rightarrow T_c = 0.3\,K$

But real $T_c = 1043\,K$

iv) understanding magnetic moments of 3d-shell and 4f-shell atoms

⇒ use quantum mechanical rules for combining $\vec{J} = \vec{L} + \vec{S}$ + Hund's rules that specify which states are preferred energetically

- FIRST RULE → spin state is such that total spin is maximized
- SECOND RULE → occupation of l_z should maximize L
- THIRD RULE → $J = |L-S|$ when electronic shell is half filled $n \le 2l+1$, and $J = L+S$ for $n \ge 2l+1$

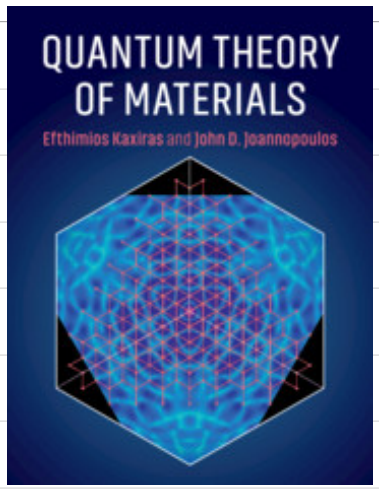

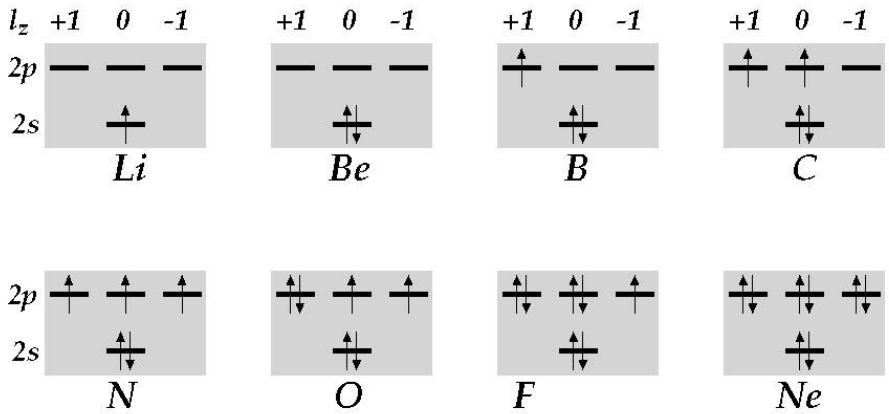

Figure 7.1. Schematic representation of the filling of the $2s$ and $2p$ electronic shells by electrons according to Hund's rules. The resulting total spin and orbital angular momentum values are: Li:$(S=\frac{1}{2}, L=0)$, Be:$(S=0, L=0)$, B:$(S=\frac{1}{2}, L=1)$, C:$(S=1, L=1)$, N:$(S=\frac{3}{2}, L=0)$, O:$(S=1, L=1)$, F:$(S=\frac{1}{2}, L=1)$, Ne:$(S=0, L=0)$.

Table 7.1. *Atomic spin states according to Hund's rules.*

Total spin S, orbital angular momentum L and total angular momentum J numbers for the $l=2$ (d shell) and $l=3$ (f shell) as they are being filled by n electrons, where $1 \le n \le 2(2l+1)$. Of the two expressions for J, the $-$ sign applies for $n \le (2l+1)$ and the $+$ sign applies for $n \ge (2l+1)$. The standard spectroscopic symbols, ${}^{(2S+1)}X_J$, are also given with $X = S, P, D, F, G, H, I$ for $L = 0, 1, 2, 3, 4, 5, 6$. For the $3d$-shell transition metals and the $4f$-shell rare earth elements we give the calculated (p_{th}) and experimental (p_{exp}) values of the effective Bohr magneton number; note the ionization of the various elements (right superscript) which makes them correspond to the indicated state.

$p_{th} = g_J\sqrt{J(J+1)}$

l	n	$S=\lvert\sum s_z\rvert$	$L=\lvert\sum l_z\rvert$	$J=\lvert L \mp S\rvert$	${}^{(2S+1)}X_J$		p_{th}	p_{exp}
2	1	1/2	2	3/2	${}^2D_{3/2}$	Ti^{3+}	1.73[a]	1.8
2	2	1	3	2	${}^3F_2$	V^{3+}	2.83[a]	2.8
2	3	3/2	3	3/2	${}^4F_{3/2}$	Cr^{3+}	3.87[a]	3.7
2	4	2	2	0	${}^5D_0$	Mn^{3+}	4.90[a]	5.0
2	5	5/2	0	5/2	${}^6S_{5/2}$	Fe^{3+}	5.92[a]	5.9
2	6	2	2	4	${}^5D_4$	Fe^{2+}	4.90[a]	5.4
2	7	3/2	3	9/2	${}^4F_{9/2}$	Co^{2+}	3.87[a]	4.8
2	8	1	3	4	${}^3F_4$	Ni^{2+}	2.83[a]	3.2
2	9	1/2	2	5/2	${}^2D_{5/2}$	Cu^{2+}	1.73[a]	1.9
2	10	0	0	0	${}^1S_0$	Zn^{2+}	0.00	
3	1	1/2	3	5/2	${}^2F_{5/2}$	Ce^{3+}	2.54	2.4
3	2	1	5	4	${}^3H_4$	Pr^{3+}	3.58	3.5
3	3	3/2	6	9/2	${}^4I_{9/2}$	Nd^{3+}	3.62	3.5
3	4	2	6	4	${}^5I_4$	Pm^{3+}	2.68	
3	5	5/2	5	5/2	${}^6H_{5/2}$	Sm^{3+}	0.84	1.5
3	6	3	3	0	${}^7F_0$	Eu^{3+}	0.00	3.4
3	7	7/2	0	7/2	${}^8S_{7/2}$	Gd^{3+}	7.94	8.0
3	8	3	3	6	${}^7F_6$	Tb^{3+}	9.72	9.5
3	9	5/2	5	15/2	${}^6H_{15/2}$	Dy^{3+}	10.63	10.6
3	10	2	6	8	${}^5I_8$	Ho^{3+}	10.60	10.4
3	11	3/2	6	15/2	${}^4I_{15/2}$	Er^{3+}	9.59	9.5
3	12	1	5	6	${}^3H_6$	Tm^{3+}	7.57	7.3
3	13	1/2	3	7/2	${}^2F_{7/2}$	Yb^{3+}	4.54	4.5
3	14	0	0	8	${}^1S_0$	Lu^{3+}	0.00	

3d

4f

[a] Values obtained from the quenched total angular momentum expression ($L=0 \Rightarrow J=S$) which are in much better agreement with experiment than those from the general expression, Eq. (7.8). Source: [74].

V) Exchange interaction between magnetic moments is effective way to describe combined effect of Coulomb interaction and symmetrization postulate in orbital space

A • e⁻ e⁻ • B → consider two atoms with one valence e⁻ per atom

$$\hat{H} = \hat{H}_0 + \hat{H}'$$

$$\hat{H}_0 = -\hbar^2\nabla_1^2/2m + W(\vec{r}_1-\vec{R}_A) - \hbar^2\nabla_2^2/2m + W(\vec{r}_2-\vec{R}_B)$$

$$\hat{H}' = W(\vec{r}_2-\vec{R}_A) + W(\vec{r}_1-\vec{R}_B) + V(\vec{r}_1-\vec{r}_2)$$

$V(\vec{r}_1-\vec{r}_2) = e^2/4\pi\varepsilon_0|\vec{r}_1-\vec{r}_2|$

→ try perturbation approach:

$$\hat{H}_0\,\phi_j(\vec{r}_1-\vec{R}_A)\,\phi_k(\vec{r}_2-\vec{R}_B) = (\varepsilon_j+\varepsilon_k)\,\phi_j(\vec{r}_1-\vec{R}_A)\,\phi_k(\vec{r}_2-\vec{R}_B)$$

↳ separable Hamiltonian $\hat{H}_{0,1}\otimes\hat{I}_2 + \hat{I}_1\otimes\hat{H}_{0,2}$ where

$$\left[\hat{H}_{0,1} = \hat{H}_{0,2} = -\frac{\hbar^2\nabla^2}{2m} + W(\vec{r})\right]\phi_j(\vec{r}) = \varepsilon_j\,\phi_j(\vec{r})$$

but this fails → WHY?

→ try variational approach with trial wavefunction:

$$\psi_\pm(\vec{r}_1,\vec{r}_2) = \phi_A(1)\,\phi_B(2) \pm \phi_B(1)\,\phi_A(2)$$ ← not eigenstate of $\hat{H}_0$

$$E_\pm = \frac{\langle\psi_\pm|\hat{H}|\psi_\pm\rangle}{\langle\psi_\pm|\psi_\pm\rangle}$$

↳ $\phi_A(1) = \phi(\vec{r}_1-\vec{R}_A)$

↳ $\phi_B(2) = \phi(\vec{r}_2-\vec{R}_B)$

$$\langle \phi_A | \phi_A \rangle = \langle \phi_B | \phi_B \rangle = 1 \Rightarrow \langle \psi_\pm | \psi_\pm \rangle = 2\left(1 \pm |\langle \phi_A | \phi_B \rangle|^2\right)$$

$$E_\pm = \frac{\langle \phi_A(1)\phi_B(2)|\hat{H}|\phi_A(1)\phi_B(2)\rangle \pm \langle \phi_A(1)\phi_B(2)|\hat{H}|\phi_B(1)\phi_A(2)\rangle}{1 \pm |\langle \phi_A|\phi_B\rangle|^2}$$

$\langle \phi_A | \phi_B \rangle \ll 1 \Rightarrow E_+ - E_- \approx 2K$

$$\langle \hat{V} \rangle = \frac{\langle \psi_\pm | \hat{V} | \psi_\pm \rangle}{\langle \psi_\pm | \psi_\pm \rangle} \approx C \pm K$$

expectation value of Coulomb interaction if positions of two e^- are statistically independent

$$C = \int\int |\phi(\vec{r}_1 - R_A)|^2 |\phi(\vec{r}_2 - \vec{R}_B)|^2 V(\vec{r}_1 - \vec{r}_2)\, d^3r_1 d^3r_2$$

$$K = \int\int \phi^*(\vec{r}_1 - \vec{R}_A)\phi^*(\vec{r}_2 - \vec{R}_B) \cdot V(\vec{r}_1 - \vec{r}_2)\phi(\vec{r}_1 - \vec{R}_B)\phi(\vec{r}_2 - \vec{R}_A) d^3r_1 d^3r_2$$

→ although $\psi_\pm$ are approximate wavefunctions, true eigenfunctions will also be symmetric or antisymmetric with corresponding difference in eigenenergies $E_\pm$

$\in \mathcal{H}_1^o \otimes \mathcal{H}_2^o$

$$\hat{H}|\psi_\pm\rangle \otimes |\text{spin}\rangle = E_\pm |\psi_\pm\rangle \otimes |\text{spin}\rangle \in \mathcal{H}_1^s \otimes \mathcal{H}_2^s$$

or

$$|\psi_\pm\rangle \otimes \hat{H}_{\text{eff}}|\text{spin}\rangle = E_\pm |\psi_\pm\rangle \otimes |\text{spin}\rangle$$

$\frac{1}{2}\vec{\hat{\sigma}}_1 \leftrightarrow \vec{\hat{S}}_1 \quad \vec{\hat{S}}_2 \leftrightarrow \frac{1}{2}\vec{\hat{\sigma}}_2$

$$\hat{H}_{\text{eff}} = a - b\,\vec{\hat{S}}_1 \cdot \vec{\hat{S}}_2 \; ; \; a = (E_+ + 3E_-)/4, \; b = E_+ - E_-$$

→ we can use spin-dependent effective Hamiltonian only because the symmetrization postulate correlates a symmetric spatial wavefunction with an antisymmetric spin state, and vice versa

QUIZ: $\vec{\hat{\sigma}}_1 \cdot \vec{\hat{\sigma}}_2 |\text{singlet}\rangle = ? |\text{singlet}\rangle$

$\vec{\hat{\sigma}}_1 \cdot \vec{\hat{\sigma}}_2 |\text{triplet}\rangle = ? |\text{triplet}\rangle$

$b > 0 \Rightarrow$ triplet has lowest energy, so ferromagnetism ↑↑

$b < 0 \Rightarrow$ singlet has lowest energy, so antiferromagnetism ↑↓

vi) Heisenberg Hamiltonian

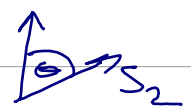

→ two classical spins $\quad H = -J\,\vec{S}_1 \cdot \vec{S}_2$

$$E = -\frac{1}{4} J \cos\theta \in \left[-\frac{1}{4}J, \frac{1}{4}J\right]$$

→ two quantum spin-$\frac{1}{2}$ described in $\mathcal{H}_1^S \otimes \mathcal{H}_2^S$

$$\hat{H} = -J\,\hat{\vec{S}}_1 \cdot \hat{\vec{S}}_2 = -J\left(\hat{S}_x \otimes \hat{S}_x + \hat{S}_y \otimes \hat{S}_y + \hat{S}_z \otimes \hat{S}_z\right)$$

$$= -\begin{pmatrix} 1/4 & 0 & 0 & 0 \\ 0 & -1/4 & 1/2 & 0 \\ 0 & 1/2 & -1/4 & 0 \\ 0 & 0 & 0 & 1/4 \end{pmatrix} \begin{matrix} |\uparrow\uparrow\rangle \\ |\uparrow\downarrow\rangle \\ |\downarrow\uparrow\rangle \\ |\downarrow\downarrow\rangle \end{matrix}$$

$|\uparrow\uparrow\rangle \; |\uparrow\downarrow\rangle \; |\downarrow\uparrow\rangle \; |\downarrow\downarrow\rangle$

much longer than classical maximum

triple degeneracy

$$\hat{H}\,|E_{1,2}\rangle = E_{1,2}\,|E_{1,2}\rangle \;;\; E_1 = -J/4 \;,\; E_2 = 3J/4$$

eigenstate no.	ket	intuition	S_{total}	S^z_{total}	E eigenvalue	
1	$\|\uparrow\uparrow\rangle$	$\uparrow\uparrow$	1	1	$-J/4$	$\}$ $\|E_1\rangle$ triplet
2	$\frac{1}{\sqrt{2}}(\|\uparrow\downarrow\rangle + \|\downarrow\uparrow\rangle)$	$\rightarrow\rightarrow$	1	0	$-J/4$	
3	$\|\downarrow\downarrow\rangle$	$\downarrow\downarrow$	1	-1	$-J/4$	
4	$\frac{1}{\sqrt{2}}(\|\uparrow\downarrow\rangle - \|\downarrow\uparrow\rangle)$	$\uparrow\downarrow$	0	0	$3J/4$	$\}$ $\|E_2\rangle$ singlet

$$\vec{S}_{total} = \vec{S}_1 + \vec{S}_2 \;;\; \hat{S}^2_{total} = \left(\hat{S}^x_{total}\right)^2 + \left(\hat{S}^y_{total}\right)^2 + \left(\hat{S}^z_{total}\right)^2$$

$$[\hat{H}, \hat{S}^x_{total}] = [\hat{H}, \hat{S}^y_{total}] = [\hat{H}, \hat{S}^z_{total}] = 0$$

$$[\hat{H}, \hat{S}^2_{total}] = 0$$

$$\hat{H} = -J \sum_{\langle ij \rangle}{}' \vec{\hat{S}}_i \cdot \vec{\hat{S}}_j - g\mu_B \vec{h}_{ext} \cdot \sum_{i=1}^{N}{}' \vec{\hat{S}}_i$$

spontaneous symmetry breaking $\Leftrightarrow$ ground state has lower symmetry than $\hat{H}$ itself

$\hat{H}$ acts in $\mathcal{H}_1^S \otimes \cdots \otimes \mathcal{H}_N^S$

GS

- $J > 0 \Rightarrow$ ground state is ferromagnetic

$\uparrow\uparrow\uparrow\cdots\uparrow$ classical GS

$|GS\rangle = |\uparrow\uparrow\uparrow\cdots\uparrow\rangle \equiv |\uparrow\rangle \otimes |\uparrow\rangle \otimes \cdots \otimes |\uparrow\rangle$ quantum GS

z: no. of nearest neighbors

$$E_0 = \langle GS | \hat{H} | GS \rangle = -J |S|^2 N z/2$$

$$\hat{S}_z^{\text{total}} |GS\rangle = SN |GS\rangle$$

$S \to \infty$

$S = 1/2$ or 1 is "ultraquantum" limit

$\hat{S}^2$ has eigenvalues $S(S+1) = S^2(1 + 1/S)$ instead of classical S^2, so as $S \to \infty$ correction factor $1 + 1/S$ due to quantum nature of spins goes to 1

- $J < 0 \Rightarrow$ ground state is antiferromagnetic

$\uparrow\downarrow\uparrow\downarrow\cdots\uparrow\downarrow$ classical (Néel) GS

$|GS\rangle \neq |\uparrow\downarrow\uparrow\downarrow\cdots\uparrow\downarrow\rangle$ due to "quantum spin fluctuations" or "zero point motion"

what does this mean RIGOROUSLY?

→ diagonalize Hamiltonian of a simple 1D chain of 4 spins:

$$\langle \uparrow\downarrow\uparrow\downarrow | \hat{H} | \uparrow\downarrow\uparrow\downarrow \rangle = -|J| \quad > \quad \langle GS | \hat{H} | GS \rangle = -2|J|$$

(true GS has lower energy)

$$|GS\rangle = \frac{1}{\sqrt{12}} \big(2|\uparrow\downarrow\uparrow\downarrow\rangle + 2|\downarrow\uparrow\downarrow\uparrow\rangle - |\uparrow\uparrow\downarrow\downarrow\rangle - |\uparrow\downarrow\downarrow\uparrow\rangle - |\downarrow\downarrow\uparrow\uparrow\rangle - |\downarrow\uparrow\uparrow\downarrow\rangle \big)$$

■ magnons as low-energy excitations above GS

→ $|\ell\rangle \equiv |\uparrow\uparrow\uparrow \cdots \downarrow\uparrow \cdots \uparrow\rangle$ with spin flipped at site ℓ

$|\downarrow\uparrow\uparrow\cdots\uparrow\rangle$ or $|\downarrow\downarrow\uparrow\uparrow\cdots\uparrow\rangle$ are NOT eigenstates of $\hat{H}$

$\hat{S}^z_{total}|\downarrow\uparrow\uparrow\cdots\uparrow\rangle = (SN-1)|\downarrow\uparrow\uparrow\cdots\uparrow\rangle$ is eigenstate of $\hat{S}_z$

↳ once a single spin-flip at a particular site is created, the flipped spin state on its neighbor is also possible:

so $\hat{H}$ is diagonalized by $\hat{H}|q\rangle = [E_0 + \underbrace{2JS(1-\cos q)}_{\omega_q \approx 2JSq^2}]|q\rangle$

magnon → $|q\rangle = \frac{1}{\sqrt{N}}\sum_\ell e^{iq\ell}|\ell\rangle$ as collective bosonic excitation carrying spin 1x $\hbar$ at small $q \to 0$

$\hat{S}^z_i|q\rangle = \hbar(S - \frac{1}{N})|q\rangle$

↳ local spin deviation in one-magnon state shows reduction of the z-component of each spin by $1/N$ thereby justifying

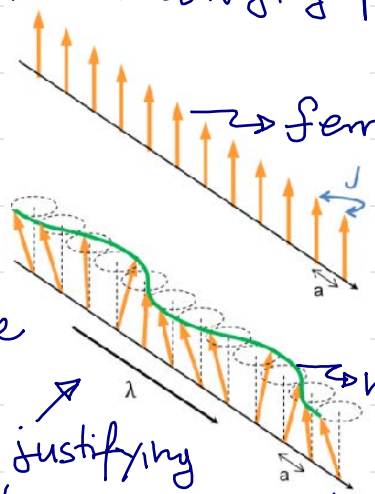

→ ferromagnetic ground state

total spin of FM reduced by

$\hat{S}^z_{total}|q\rangle = \hbar(SN-1)|q\rangle$

→ magnon or spin wave

→ BETHE ANSATZ: $S = 1/2$ is integrable, i.e., EXACTLY SOLVABLE where he was able to start from $S^z_{total} = \frac{N}{2} - 3$ and construct eigenstates $S^z_{total} = \frac{N}{2} - r$

■ Mermin-Wagner theorem PROOF: Divergent magnon number in 1D & 2D

$$m = \frac{1}{N}\sum_i \langle \hat{S}_i^z\rangle = S - \frac{1}{N}\sum_i \langle n_i\rangle = S - \frac{1}{N}\sum_{\vec{q}} \langle n_{\vec{q}}\rangle = S - \delta m$$

$$\delta m \xrightarrow{\text{1D \& 2D FM}} \frac{1}{N}\left(\sum_{q_0 < |\vec{q}| < \bar{q}} \frac{1}{e^{\beta 2JSq^2} - 1} + \sum_{|\vec{q}| > \bar{q}} \frac{1}{e^{\beta\omega_{\vec{q}}} - 1}\right)$$

$\omega_{\bar{q}} \ll k_BT \ll 2JS\bar{q}^2$

$$\int_{q_0}^{\bar{q}} dq\, q^{d-1}\frac{k_BT}{JSq^2} \propto \frac{k_BT}{JS}\cdot\begin{cases} 1/q_0 + \ldots, & d=1 \\ -\ln q_0 + \ldots, & d=2 \end{cases}$$

FM + anisotropy → $\int_0^\infty dq\, q^{d-1}\frac{1}{e^{\beta(2JS^2q^2+D)}-1} = \frac{1}{\beta}e^{-\beta D}$, so finite

3D FM

$$\frac{1}{e^x-1} = \frac{e^{-x}}{1-e^{-x}} = e^{-x}\sum_{n=0}^\infty (e^{-x})^n \Rightarrow \delta m = \frac{1}{(2\pi)^3}4\pi\int_0^\infty dq\, q^2 \sum_{n=1}^\infty e^{-n\beta 2JSq^2} \approx \frac{1}{8}\left(\frac{k_BT}{2\pi JS}\right)^{3/2}\zeta\left(\frac{3}{2}\right)$$

vii) Anisotropic spin Hamiltonians: Ising and others

→ XXZ quantum Heisenberg model

$$\hat{H} = -\sum_{\langle i,j \rangle} \left(\hat{S}_i^x \cdot \hat{S}_i^x + \hat{S}_i^y \cdot \hat{S}_i^y + \Delta \hat{S}_i^z \cdot \hat{S}_i^z \right)$$

→ classical Heisenberg model with easy axis or easy plane anisotropy

$$H = -\sum_{\langle i,j \rangle} J \vec{S}_i \cdot \vec{S}_j \mp \sum_i D (S_i^z)^2$$

(− : easy axis; + : easy plane)

→ classical XY model with $S_z \equiv 0$ or "planar rotator"

$$H = -\sum_{\langle i,j \rangle} J \left(S_i^x S_i^x + S_i^y S_i^y \right) - \sum_i D (S_i^x)^2$$

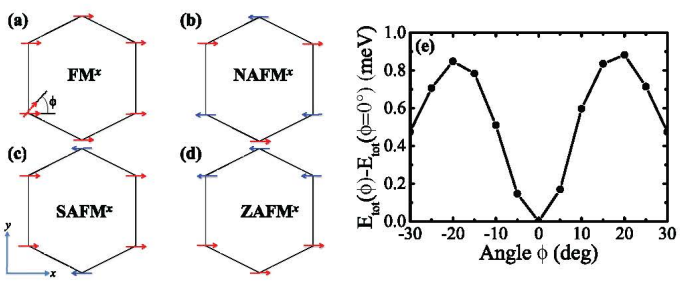

FIG. 4. Possible configurations of Os spins on the honeycomb lattice: (a) ferromagnet (FM), (b) Néel antiferromagnet (NAFM), (c) stripy AFM (SAFM), and (d) zigzag AFM (ZAFM). (e) Change of total energy E_{tot} as spins in FM^x configuration in (a) rotate within the xy plane.

TABLE II. The total energy E_{tot} per unit cell (in meV, relative to E_{tot} of FM^x ground state), as well as spin $\langle S \rangle$ and orbital $\langle O \rangle$ moments (in μ_B), for several magnetic configurations of Os atoms (first four of which are illustrated in Fig. 4) calculated by GGA+SOC method. Paramagnetic state has $E_{\text{tot}} = 47.36$ meV and $\langle S \rangle = \langle O \rangle = 0$.

	FM^x	NAFM^x	SAFM^x	ZAFM^x	FM^z	FM^y	NAFM^y
E_{tot}	0.0	39.60	47.57	16.63	27.42	0.51	39.61
$\langle S \rangle$	0.57	0.13	0.10	0.41	0.30	0.57	0.13
$\langle O \rangle$	0.30	0.24	0.90	0.33	0.12	0.30	0.24

ically favorable magnetization directions (such as easy-axis, easy-plane or easy-cone) and determines stability of that direc-

→ quantum Ising model in transverse magnetic field

$$\hat{H} = -J \sum_{\langle i,j \rangle} \hat{\sigma}_i^z \otimes \hat{\sigma}_i^z - h \sum \hat{\sigma}_i^x$$

→ used in the study of quantum phase transitions

→ classical Ising model → favorite of SM textbooks

$$H = -J \sum_{\langle i,j \rangle} S_i \cdot S_j - h \sum S_i$$

$m = \langle S_i \rangle$ is order parameter

for $h = 0$ it is invariant under $S \to -S_i \Rightarrow$ discrete $\mathbb{Z}_2$ symmetry

Box 1 | Examples of magnetic configurations of vdW layered materials

The strong geometrical anisotropy of vdW layered crystals—which leads to a significant difference in magnitude between intralayer (J) and interlayer (J_L) exchange coupling—also manifests itself in different kinds of interlayer spin alignment found in different material systems. Here we illustrate different examples, along with experimentally reported materials realizations. Semiconducting and metallic compounds are distinguished with different colours; the scheme does not illustrate the magnetic anisotropy of the different materials (for instance, in the bottom right quadrant, CrI_3 and $CrCl_3$ are both layered antiferromagnets with all spins ferromagnetically ordered in each plane, but whereas in CrI_3 the layer magnetization points perpendicular to the plane, in $CrCl_3$ it lies in the plane)[118–127].

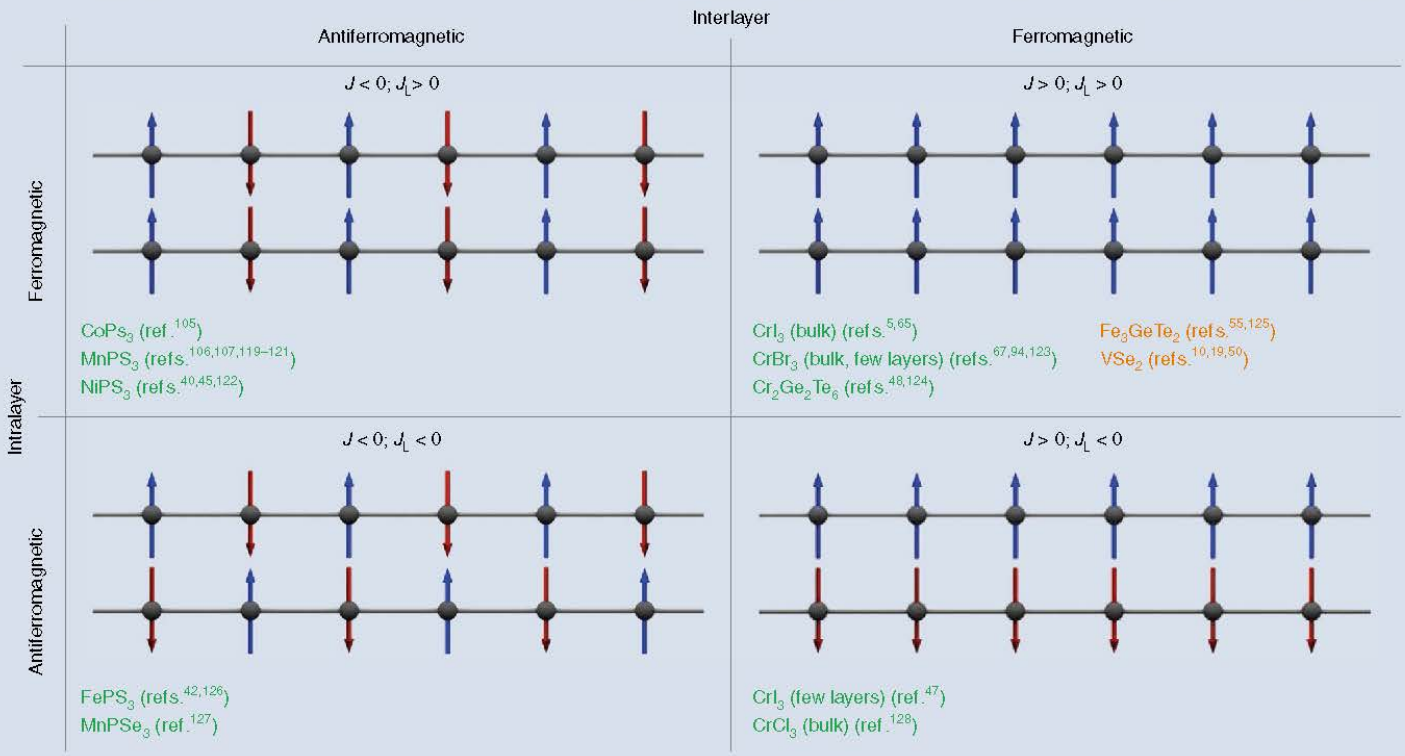

→ Hopfield neural network as content-addressable or "associative" memory

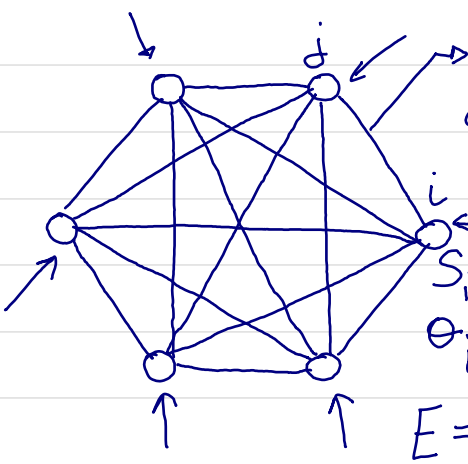

w_{ij} is strength of i–j connection

I_i is input

S_i is state

θ_i is threshold

$$S_i = \begin{cases} +1, & \sum_j w_{ij} S_j > \theta_i \\ -1, & \text{otherwise} \end{cases}$$

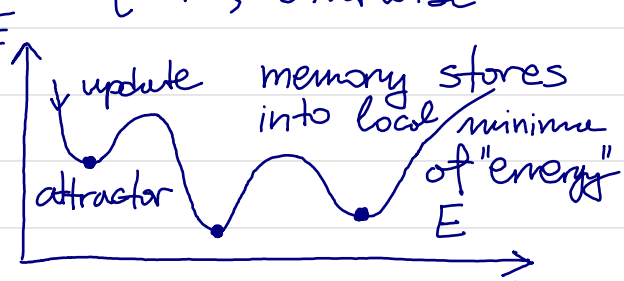

$$E = -\frac{1}{2}\sum_{i,j} w_{ij} S_i S_j - \sum_i I_i S_i - \sum_i \theta_i S_i$$

4° Correlation function

$$G(r) \overset{\text{def}}{=} \underbrace{\langle S_i S_{i+r} \rangle}_{m} - \underbrace{\langle S_i \rangle \langle S_{i+r} \rangle}_{m} \leftarrow \text{Ising model}$$

$$= \langle (S_i - \langle S_i \rangle)(S_{i+r} - \langle S_{i+r} \rangle) \rangle$$

↳ measures degree of similarity of Ising spins separated by distance r

$$G(\vec{r}-\vec{r}') = \langle m(\vec{r}) m(\vec{r}') \rangle - \langle m(\vec{r}) \rangle \langle m(\vec{r}') \rangle \leftarrow \text{continuous local magnetization}$$

$\lim_{h\to 0} \lim_{N\to\infty} m(h) \neq 0$ in ferromagnetic phase

$\lim_{h\to 0} \lim_{|\vec{r}-\vec{r}'|\to\infty} \lim_{N\to\infty} \langle S_i S_j \rangle \neq 0$; $G(r) \propto \frac{1}{r^{d-2+\eta}} e^{-r/\xi}$, $T \neq T_c$

correlation between spins is small beyond distance ξ called correlation length, except at T_c

■ Fluctuation-dissipation theorem connecting $G(r)$ with $\chi(r)$

$$M = \frac{\sum_{\{S_i\}} (S_1 + S_2 + \dots + S_N) e^{-\beta H_0 + \beta h \sum' S_i}}{\sum_{\{S_i\}} e^{-\beta H_0 + \beta h \sum_i S_i}}, \quad H_0 = -J \sum'_{\langle i,j \rangle} S_i \cdot S_j$$

$$N\chi = \lim_{h\to 0} \frac{\partial M}{\partial h} = \frac{\beta \sum_{\{S_i\}} (S_1 + \dots + S_N)^2 e^{-\beta H_0}}{\sum_{\{S_i\}} e^{-\beta H_0}}$$

$$- \beta \left(\frac{\sum_{\{S_i\}} (S_1 + \dots + S_N) e^{-\beta H_0}}{\sum_{\{S_i\}} e^{-\beta H_0}} \right)^2$$

↑ susceptibility per spin

$$N\chi = \beta \sum_{i,j=1}^{N} \langle S_i S_j \rangle - \beta M^2$$

$\langle S_i S_j \rangle = \langle S_0 S_r \rangle$ in translationally invariant system

$r = |i-j|$

$\langle S_i \rangle = M/N = m$

$$\chi = \beta \sum_i \underbrace{\left(\langle S_0 S_i \rangle - \langle S_0 \rangle \langle S_i \rangle \right)}_{G(i)}$$

↳ so susceptibility is the sum of correlation functions

$k_B T \chi < g \cdot \xi^2$

↳ typical value of correlation function for $r < \xi$

$\chi \to \infty$ at $T \to T_c$ requires $\xi \to \infty$

$\xi_{\pm} = |t|^{-\nu_{\pm}}$ for $|t| \to 0\pm$

so, divergent correlation length is behind all phenomena at T_c including critical opalescence observed experimentally

$$G(r) = \frac{1}{r^{d-2+\eta}} \quad \text{at } T = T_c$$

η: anomalous dimension

d: dimension of space

5° Criticality and power laws in complex systems, including BRAIN

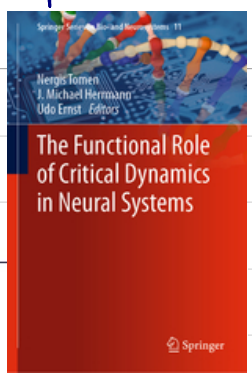

Physics

Viewpoint

The Critical Brain

Dietmar Plenz
Section on Critical Brain Dynamics, National Institute of Mental Health, NIH, Bethesda, MD 20892, USA

Published April 22, 2013

A model describing the brain as a system close to a phase transition can capture the global dynamics of brain activity observed in fMRI experiments.

Subject Areas: Biological Physics

frontiers in PHYSIOLOGY

REVIEW ARTICLE
published: 07 June 2012
doi: 10.3389/fphys.2012.00163

Being critical of criticality in the brain

John M. Beggs[1,2] and Nicholas Timme[1]*

[1] Department of Physics, Indiana University, Bloomington, IN, USA
[2] Biocomplexity Institute, Indiana University, Bloomington, IN, USA

Edited by:
Tjeerd W. Boonstra, University of New South Wales, Australia

Reviewed by:
Alain Destexhe, Information and Complexité Centre National de la Recherche Scientifique, France
Woodrow Shew, University of Arkansas, USA

***Correspondence:**
John M. Beggs, Department of Physics, Indiana University, 727 East, 3rd Street, Bloomington, IN 47405-7105, USA.
e-mail: jmbeggs@indiana.edu

Relatively recent work has reported that networks of neurons can produce avalanches of activity whose sizes follow a power law distribution. This suggests that these networks may be operating near a critical point, poised between a phase where activity rapidly dies out and a phase where activity is amplified over time. The hypothesis that the electrical activity of neural networks in the brain is critical is potentially important, as many simulations suggest that information processing functions would be optimized at the critical point. This hypothesis, however, is still controversial. Here we will explain the concept of criticality and review the substantial objections to the criticality hypothesis raised by skeptics. Points and counter points are presented in dialog form.

Keywords: criticality, scale-free, avalanche, network, multi-electrode array, statistical physics, Ising model

A Viewpoint on:
Brain Organization into Resting State Networks Emerges at Criticality on a Model of the Human Connectome
Ariel Haimovici, Enzo Tagliazucchi, Pablo Balenzuela, and Dante R. Chialvo
Phys. Rev. Lett. 110, 178101 (2013) – Published April 22, 2013

Critical systems can be defined as systems that are close to a critical point, generally identified as the boundary of an order-disorder phase transition. Many complex systems far from equilibrium and composed of a large number of interacting elements have been successfully modeled as critical: notable examples range from gene-interaction networks to financial markets. At criticality, these systems can avoid being trapped in one of two extreme cases: a disordered state (when interactions are too weak and the system is dominated by noise) or a globally ordered state in which all elements are locked (when interactions are too strong and the system is completely static). Neither state supports the dualism essential for a complex system like the brain to function: it must maintain some order to ensure coherent functioning (i.e., generate a reproducible behavior in response to a certain stimulus) while allowing for a certain degree of disorder to enable flexibility (i.e., adapt to varying external conditions). Such dualism is instead possible at criticality.

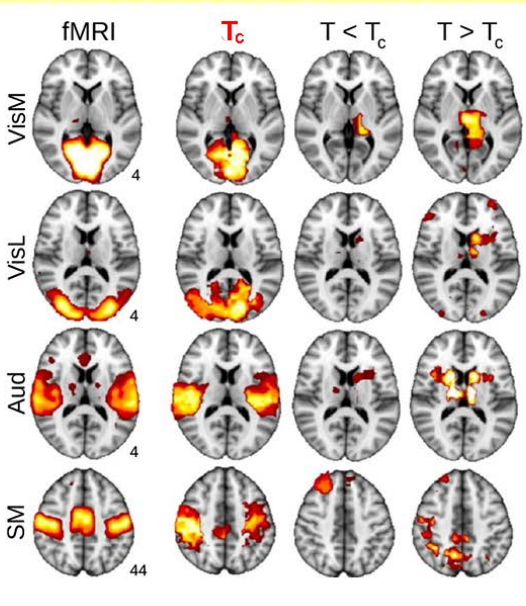

FIG. 1: (Left column) Functional magnetic resonance imaging (fMRI) experiments have revealed that the brain at rest is organized into several areas in which fluctuations of brain activities are correlated, so-called resting state networks (RSN). From top to bottom: Medial visual (VisM), lateral visual (VisL), auditory (Aud), and sensory-motor (SM) RSNs. (Right columns) Results from the work of Haimovici *et al.*[1] show that a simple model can reproduce the statistical properties of RSNs only if the model is tuned to criticality (at T_C). (A. Haimovici *et al.*, Phys. Rev. Lett. (2013))

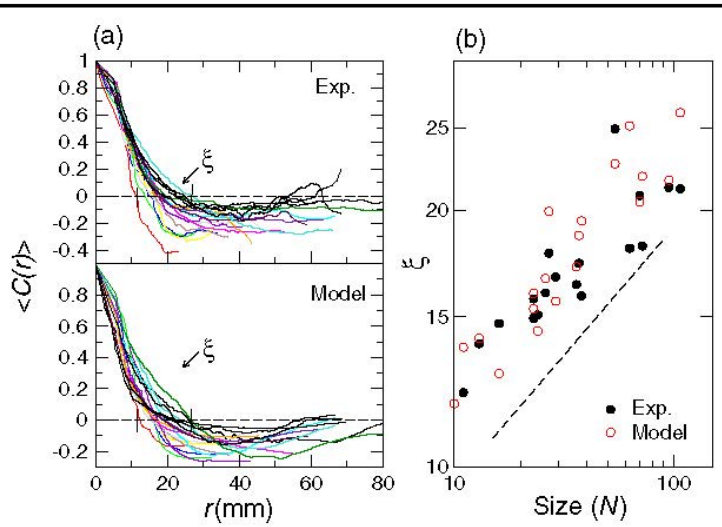

FIG. 2 (color online). The correlation length ξ of the activity in the model near T_c increases with the cluster size (N), as reported for human brain data [17]. Panel (a) shows the correlation function $C(r)$ computed from human data (Exp) and from the model at T_c (colored lines are used for the different clusters). The correlation length ξ is the distance r where $C(r) = 0$, (range denoted with the arrows). Panel (b) shows the ξ values for the functions plotted on panel (a), demonstrating that $\xi \sim N^{1/3}$ (dashed line), both in the experiment and model data.